Study of the U–Zr–O Ternary System*

S. YAMANAKA, M. KATSURA, S. IMOTO
and M. MIYAKE†

Department of Nuclear Engineering, Faculty of Engineering, Osaka University, Yamadaoka 2–1, Suita, Osaka 565, Japan

In recent years, high-temperature interactions between UO_2 fuel and Zircaloy cladding have been studied to elucidate the fuel rod behavior under severe core damage conditions. Interfacial reaction of UO_2 with Zircaloy has been extensively investigated from kinetic points of view [1–3], and several analytical models have been proposed for the reaction [4–6].

For an understanding of the UO_2/Zircaloy chemical interaction, information is needed both on the reaction kinetics and on phase equilibria in a U–Zr–O ternary system. The UO_2/Zircaloy interaction cannot be explained in terms of a pseudobinary UO_2–Zr system, but should be treated as a ternary reaction in the U–Zr–O system.

The first study of phase relations in the U–Zr–O system was made by Saller *et al.* [7], and Politis [8] has proposed the isothermal sections at 1000, 1500 and 2000 °C. In our previous papers [9, 10], the isothermal section at 1000 °C has been reconstructed in the U–Zr–O system. Skokan and coworkers [11] have performed thermal analyses on the quasi-binary section between UO_2 and oxygen-saturated α-Zr.

In order to interpret the chemical composition of the phases and the sequence of the reaction zone in the UO_2/Zircaloy chemical interaction, further investigation of phase equilibria is considered necessary. The purpose of the present study is to clarify whether or not the formation of a liquid phase can be caused by the reaction of Zr with UO_2 at high temperatures and to examine the phase regions and boundaries in the U–Zr–O ternary system.

Experimental

Powders of UO_2 (O/U ratio = 2.16), Zr (99.9 wt.% purity) and ZrO_2 (99.9 wt.% purity) were used as starting materials. These powders were well ground and then mixed in the desired proportions. The mixtures with various compositions were pelletized, and the compacts were heated at a temperature of 1400 °C for reaction periods ranging from 20 to 50 h in a vacuum below 10^{-4} Pa. After heating, the samples were rapidly cooled to room temperature.

The heated sample was powdered in a dry argon-filled glove box, and phases in the reaction products were identified by a computer-controlled X-ray diffractometer. Lattice parameters of the reaction products were evaluated from reflections according to Cohen's method.

Metallographic examination was also made for some of the samples with the aid of a scanning electron microscope (SEM) and an optical microscope. Compositions of reaction products were analysed by means of an energy dispersive X-ray analyser (EDXA).

Results and Discussion

The results for X-ray diffraction analysis of pellets of Zr/UO_2 mixtures (samples **A**–**Y**) and Zr/ZrO_2/UO_2 mixtures (samples **a**–**x**) heated at 1400 °C are given in Fig. 1. No change with reaction period in the type and number of phases identified in the heated pellets was observed. All the results for X-ray diffraction analysis described in the present paper were

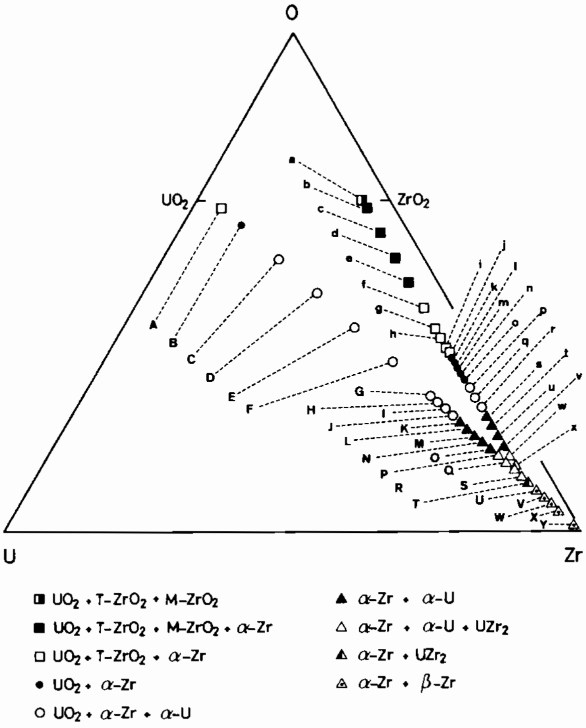

Fig. 1. Reaction products in Zr/UO_2 and Zr/ZrO_2/UO_2 mixture pellets after heating at 1400 °C.

---

*Paper presented at the Second International Conference on the Basic and Applied Chemistry of f-Transition (Lanthanide and Actinide) and Related Elements (2nd ICLA), Lisbon, Portugal, April 6–10, 1987.

†Author to whom correspondence should be addressed.

0020-1693/87/$3.50

obtained for samples with a 20-h reaction period. It is apparent from Fig. 1 that the type and number of phases are strongly dependent upon the composition of the sample.

For Zr/UO_2 mixture pellets after heating at 1400 ℃, only sample **A** was found to contain ZrO_2 in the reaction products. The X-ray diffraction pattern for sample **B** revealed that two phases (UO_2 and α-Zr) existed in the reaction products. Three phases (UO_2, α-Zr and α-U) were detected in the samples **C**–**J** with Zr contents of the samples from 20 to 66 at%. The reaction products for the samples **K**–**T** were composed of α-U and/or UZr_2 in addition to α-Zr, but UO_2 was not detected. The diffraction analysis for the samples **U**–**Y** showed that the reaction products consisted of α-Zr and β-Zr. The α-U, β-Zr and UZr_2 detected in the reaction products by X-ray diffraction analysis at room temperature are inferred to result from (U, Zr) liquid or solid solution at 1400 ℃.

The reaction products for sample **a** were composed of UO_2 and ZrO_2. In the composition range for samples **b**–**j**, UO_2, α-Zr and ZrO_2 were identified in the reaction products. The X-ray diffraction patterns of samples **a**–**e** indicated that monoclinic ZrO_2 was involved in addition to the tetragonal phase. The monoclinic ZrO_2 is presumed to be a transformed phase based on the literature of UO_2–ZrO_2 and Zr–O binary systems [12, 13], and the stable form ZrO_2 at 1400 ℃ seems to be tetragonal. UO_2 and α-Zr were present in the reaction products of samples **k**–**o**. In the samples **p**, **q** and **r**, UO_2, α-Zr and α-U were detected, while no formation of UO_2 was observed for the samples s–x.

The dependence of lattice parameters a and c, and axial ratio c/a on the Zr content of α-Zr in the reaction products of the Zr/UO_2 mixture pellet is illustrated in Fig. 2. The lattice parameters for α-Zr in the reaction products increased from $a = 0.3233$ nm and $c = 0.5149$ nm for the starting Zr powder to the values of $a = 0.3252$–0.3246 nm and $c = 0.5176$–0.5195 nm for samples **C**–**V**. The axial ratio c/a for α-Zr was also larger than that before reaction (1.593). The extent of increase in the lattice parameters and axial ratio is found from this Figure to vary with the composition of the sample. Samples **C**–**J**, in which three phases of UO_2, α-Zr and α-U were detected, showed nearly constant values of $a = 0.3247$ nm and $c = 0.5194$ nm. In this composition range, the c/a ratio of 1.600 is also independent of the Zr content of the sample. Above a Zr content of 69 at%, the lattice parameter c decreased with increasing Zr content, whereas a more complicated change in the value of a was observed as the Zr content increased. The c/a ratio rapidly decreased from 1.600 to 1.593.

Figure 3 represents the variation of lattice parameters a and c, and axial ratio c/a with the Zr content of α-Zr in $Zr/ZrO_2/UO_2$ mixture pellets. The lattice

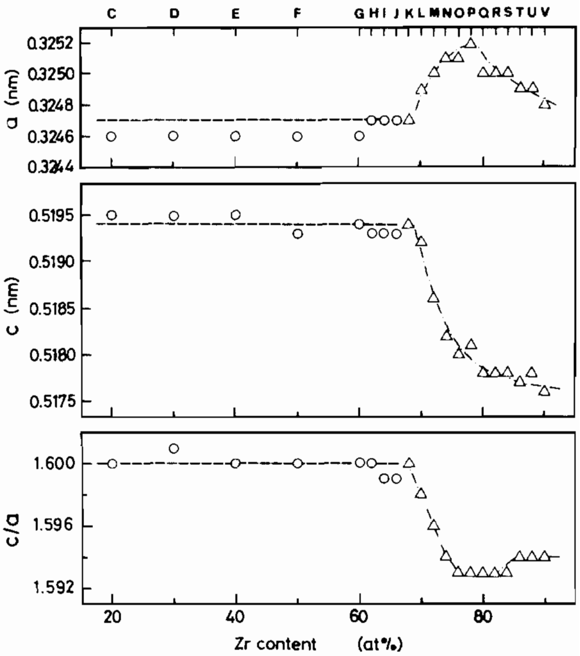

Fig. 2. Change in lattice parameters a and c, and axial ratio c/a with Zr content of α-Zr in reaction products of the Zr/UO_2 mixture pellet.

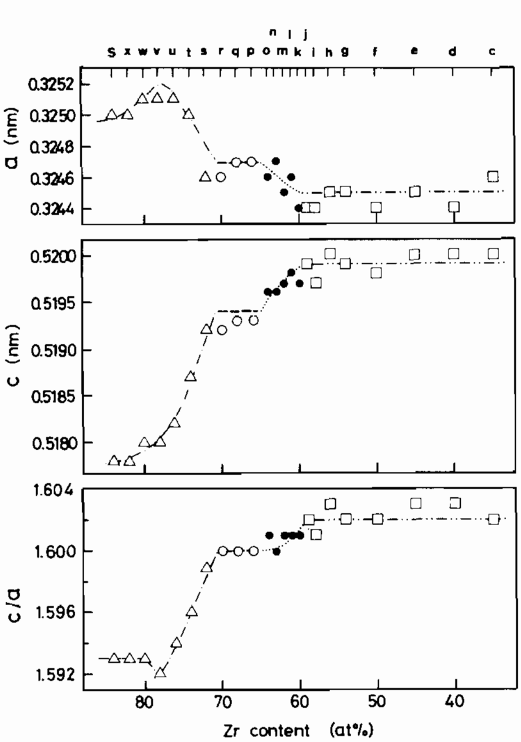

Fig. 3. Change in lattice parameters a and c, and axial ratio c/a with Zr content of α-Zr in reaction products of the $Zr/ZrO_2/UO_2$ mixture pellet.

parameters a and c and the axial ratio changed with Zr content in the range of 82–72 at% zirconium. The samples in which three phases (UO_2, α-Zr and α-U) were detected revealed nearly constant a, c and c/a values, which were close to the data for the Zr/UO_2 pellets having UO_2 as one of the reaction products. In the composition range where two phases of UO_2 and α-Zr coexisted, the lattice parameter c and the ratio c/a increased with decreasing Zr content, but the value of a decreased. There is no marked difference in values of a, c and c/a among the samples c–j with lower Zr content. The mean values of the lattice parameters and axial ratio were $a = 0.3245$ nm, $c = 0.5200$ nm, and $c/a = 1.602$.

Reaction at 1400 °C resulted in a considerable expansion in the direction of the c-axis and only a slight change in the a-axis in α-Zr. The lattice parameters of Zr and Zr–O solid solution, α-Zr(O), are provided in the literature [14–16]. The incorporation of oxygen atoms into the α-Zr lattice causes a marked increase in the value of c over the entire range of solid solubility. The value of a is less affected by the oxygen content but passes through a pronounced maximum at the composition of 20 at% oxygen. The changes in the lattice spacing after heating are considered to be closely related to oxygen dissolution in α-Zr. The lattice parameters of α-Zr in samples c–j containing ZrO_2 as one of the reaction products indicated constant values irrespective of the sample composition and were in accord with those reported for α-Zr(O) at the solubility limit of about 30 at% oxygen. Therefore, it can be concluded that in the samples c–j with UO_2 and ZrO_2 α-Zr may be saturated with oxygen. For the samples **C**–**J** and **p**–**r** which consisted of UO_2, α-Zr and α-U, α-Zr showed nearly constant lattice parameters and axial ratio, which were lower than the reported values for oxygen-saturated α-Zr(O). This suggests that α-Zr coexisting with UO_2 and α-U has a constant oxygen content and may be unsaturated with oxygen. Assuming that the solubility of uranium in α-Zr(O) is quite small and that dissolved uranium does not affect the lattice expansion of α-Zr(O), α-Zr in the reaction products for samples **C**–**J** and **p**–**r** may contain about 25 at% oxygen. However, in the composition range where no UO_2 was formed in the reaction products, the a, c and c/a values of α-Zr changed with the Zr content of the sample, and the values of c and c/a were lower than those for the samples **C**–**J** and **p**–**r**. These changes in the lattice parameters are attributed to the variation of oxygen content in α-Zr. In Zr-rich samples **K**–**V** and s–x, in which UO_2 was not identified, α-Zr appears to have various oxygen contents below 25 at% oxygen. From the results of phase identification and lattice parameter measurements, it was verified that the reduction of UO_2 by Zr produced uranium and that the type and number of phases thus formed were influenced by the composition of the sample.

Metallographic examination was carried out by means of SEM and optical microscopy for the Zr/UO_2 samples **F**, **G**, **L**, **Q**, **U**, **X** and **Y** after heating at 1400 °C for 50 h. Typical results for SEM observation are shown in Fig. 4. The samples **F** and **G** in which three phases (UO_2, α-Zr and α-U) were detected by the X-ray diffraction method were metallographically found to contain UO_2, α-Zr and metallic uranium. As evidenced by Fig. 4a, there exist large α-Zr(O) particles, and small UO_2 particles are located in the metallic region. The EDXA analysis of the metallic

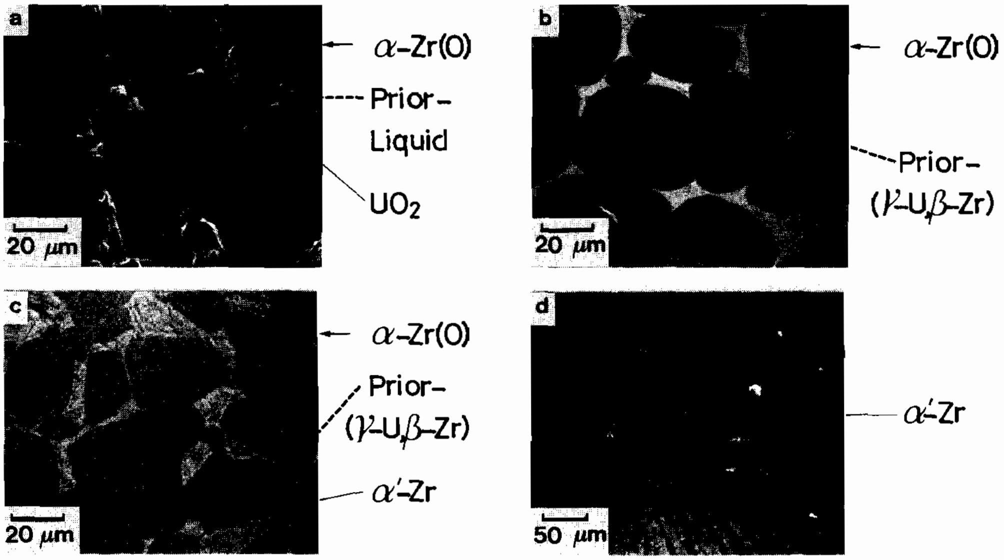

Fig. 4. Microstructures of Zr/UO_2 mixture pellets after heating at 1400 °C: (a) sample G; (b) sample L; (c) sample Q; (d) sample Y.

region revealed that the U/(U + Zr) ratio of this region was 0.95–0.90. From the morphology of this U-rich phase, it was difficult to know whether at 1400 °C the phase is liquid or not. However, the result for EDXA analysis established that on the basis of the binary phase diagram of the U–Zr system [17], the U-rich phase should be a liquid rich in uranium at 1400 °C. The uranium content in the α-Zr(O) particle was evident from EDXA analysis to be very low, and the uranium solubility in α-Zr(O) can be estimated to be below 2 at%. The samples in this composition range seem to contain three phases (UO_2, α-Zr(O) and liquid) at 1400 °C. Microstructures of samples **L** and **Q** are shown in Fig. 4b and c. In sample **L**, large α-Zr(O) particles were surrounded by a U-rich region possessing a U/(U + Zr) ratio = 0.53. The micrograph of sample **Q** indicates that the U-rich region involves needlelike α′ precipitates. The U-rich region in sample **Q** has a U/(U + Zr) ratio of 0.27. The structure of sample **U** is similar to that of sample **Q**. The value of U/(U + Zr) for the U-rich region is 0.08. For these samples, the U-rich region may exist as a (γ-U, β-Zr) solid solution at 1400 °C. In the composition range where no UO_2 was detected in the reaction products by X-ray analysis, α-Zr(O) appears to coexist with (γ-U, β-Zr) solid solution with various uranium contents. As can be seen in Fig. 4d, a number of platelike α′ precipitates were formed in prior-β-Zr matrix. This was a characteristic structure for Zr-rich samples **X** and **Y**. The α′ precipitates were introduced during cooling. Since no α-Zr(O) islands (as observed in the samples **L**, **Q** and **U**) were formed, these samples are considered to consist of a β-Zr single phase at 1400 °C.

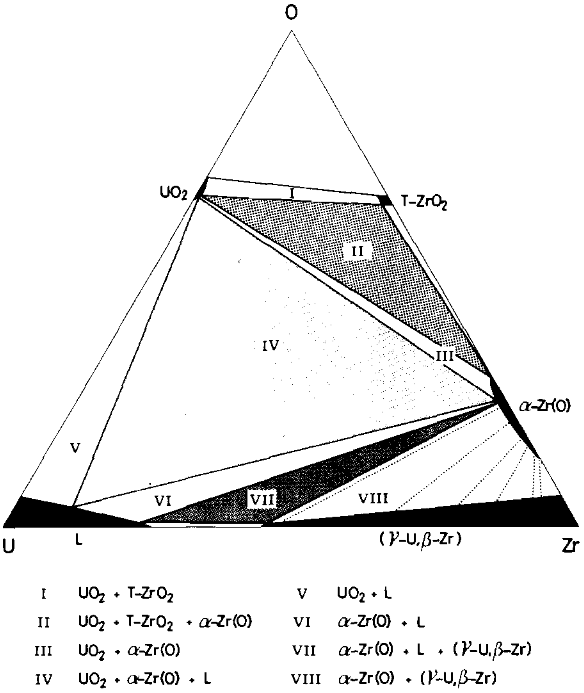

Fig. 5. Isothermal section of the U–Zr–O ternary system at 1400 °C.

Figure 5 shows the isothermal section of the U–Zr–O ternary system at 1400 °C proposed from the present results for Zr/UO_2 and $Zr/ZrO_2/UO_2$ reaction experiments. The phase relationships which differ from those obtained at lower temperatures [7–10] are essentially consistent with Politis's results at 1500 °C [8]. In the isothermal section at 1400 °C, there exists the characteristic triangle of UO_2 + α-Zr(O) + L (L = liquid). Compositions of UO_2, α-Zr(O) and liquid have to be thermodynamically fixed in this three-phase region. Actually, experimental results of lattice spacing for α-Zr in this phase region are in agreement with the phase rule. The solubilities of oxygen and uranium in α-Zr(O) are about 25 and 2 at%, respectively. The UO_2 takes little Zr into solution at 1400 °C, as can be predicted by the UO_2–ZrO_2 pseudo-binary phase diagram [12]. Although the composition of the liquid phase in equilibrium with α-Zr(O) and UO_2 was not determined precisely, it will contain about 10 at% Zr. This three-phase region may be adjacent to two-phase regions of UO_2 + L, α-Zr(O) + L, and UO_2 + α-Zr(O). In the two-phase region of UO_2 + α-Zr(O), the α-Zr(O) in equilibrium with UO_2 possesses an oxygen content ranging from 25 to 30 at%.

Compositions for samples with higher oxygen content are expected to lie in the three-phase region of UO_2, tetragonal ZrO_2 and α-Zr(O). In the two-phase region of α-Zr(O) and (γ-U, β-Zr), the lattice parameters of α-Zt vary with composition. The results for X-ray diffraction analysis of α-Zr in this region allow us to draw isoparametric lines. Tentative isoparametric lines which correspond to tie lines are shown in the isothermal section. In the binary Zr–O system, β-Zr with 6 at% oxygen content can equilibrate with 14 at% oxygen α-Zr(O) [13]. The conjugate phase of α-Zr(O) with an oxygen content of about 15 at% is likely to be a (γ-U, β-Zr) solid solution with a limited U concentration range of 0–10 at%. The compositions of (γ-U, β-Zr) in equilibrium with α-Zr(O) estimated from isoparametric lines agree with the results obtained by EDXA analysis of the Zr/UO_2 mixture pellets.

Conclusions

The isothermal section at 1400 °C was proposed for the U–Zr–O ternary system. The liquid phase was confirmed to exist in the isothermal section at 1400 °C. It should be noted that at 1400 °C UO_2 can equilibrate with α-Zr(O) of oxygen content between 25 and 30 at%. Zirconium can reduce UO_2, and may produce liquid uranium as long as the oxygen content of Zr reaches about 25 at%. However, above the oxygen content of 25 at% Zr cannot continue the oxygen absorption from UO_2.

References

1 P. Hofmann and C. Politis, *J. Nucl. Mater., 87,* 375 (1979).
2 P. Hofmann and D. Kerwin-Peck, *Report KFK-3552,* Kernforschungszentrum Karlsruhe, 1983.
3 P. Hofmann and D. Kerwin-Peck, *J. Nucl. Mater., 124,* 80 (1984).
4 A. W. Cronenberg and M. S. El-Genk, *J. Nucl. Mater., 78,* 390 (1978).
5 D. R. Olander, *J. Nucl. Mater., 115,* 271 (1983).
6 A. Denis and E. A. Garcia, *J. Nucl. Mater., 116,* 44 (1983).
7 H. A. Saller, F. A. Rough, J. M. Fackelmann, A. A. Bauer and J. R. Doigt, *Report BMI-1023,* Battelle Memorial Institute, 1955.
8 C. Politis, *Report KFK-2167,* Kernforschungszentrum Karlsruhe, 1975.
9 S. Yamanaka, M. Katsura, M. Miyake, S. Imoto and S. Kawasaki, *J. Nucl. Mater., 130,* 524 (1985).
10 S. Yamanaka, M. Katsura, S. Imoto and M. Miyake, to be published.
11 A. Skokan, K. Biemuller, G. Reiser and G. Schlickeiser, *Report KFK-3350,* Kernforschungszentrum Karlsruhe, 1983.
12 K. A. Romberger, C. F. Baes, Jr. and H. H. Stone, *J. Inorg. Nucl. Chem., 29,* 1619 (1967).
13 O. Kubaschewski, 'Zirconium', I.A.E.A., Vienna, 1976, p. 104.
14 R. F. Domagala and D. J. McPherson, *U.S.A.E.C. Publ. COO-181,* 1954.
15 B. Holmberg and T. Dagerhamn, *Acta Chem. Scand., 15,* 919 (1961).
16 P. Boisot and G. Beranger, *C.R., C, 269,* 587 (1969).
17 O. Kubaschewski, 'Zirconium', I.A.E.A., Vienna, 1976, p. 126.